REPORT DOCUMENTATION PAGE

Form Approved
OMB No. 0704-0188

PLEASE DO NOT RETURN YOUR FORM TO THE ABOVE ADDRESS.

1. REPORT DATE *(DD-MM-YYYY)*	2. REPORT TYPE	3. DATES COVERED *(From - To)*
	reprint	

4. TITLE AND SUBTITLE

Plasma-surface interactions of hydrogenated carbon

5a. CONTRACT NUMBER

W911NF-05-1-0265

5b. GRANT NUMBER

5c. PROGRAM ELEMENT NUMBER

6. AUTHOR(S)

P.S. Krstic, C.O. Reinhold, S.J. Stuart

5d. PROJECT NUMBER

W911NF-05-1-0265

5e. TASK NUMBER

5f. WORK UNIT NUMBER

7. PERFORMING ORGANIZATION NAME(S) AND ADDRESS(ES)

Thompson & Sewell Research Groups, Department of Chemistry
University of Missouri-Columbia
Columbia, MO 65211

8. PERFORMING ORGANIZATION REPORT NUMBER

9. SPONSORING/MONITORING AGENCY NAME(S) AND ADDRESS(ES)

U. S. Army Research Office
P.O. Box 12211
Research Triangle Park, NC 27709-2211

10. SPONSOR/MONITOR'S ACRONYM(S)

11. SPONSOR/MONITOR'S REPORT NUMBER(S)

48101-EG-MUR

12. DISTRIBUTION/AVAILABILITY STATEMENT

Approved for public release; federal purpose rights.

13. SUPPLEMENTARY NOTES

14. ABSTRACT

We present a review of our study of interactions of plasma particles (atoms, molecules) with hydrogenated amorphous carbon surfaces typical of plasma-facing divertor tiles and deposited layers in magnetic-fusion reactors. Our computer simulations of these processes are based on classical molecular dynamics simulations, using the best currently available multibody bond-order hydrocarbon potentials. Our research in this field has been focused on the chemical sputtering of carbon surfaces at low impact energies, the most complex of the plasma-surface interactions (PSI). Close collaboration with beam-surface and plasma-surface experiments provides not only theoretical support for the experiments, but also builds suitable benchmarks for our methods and codes, enabling production of theoretical plasma-surface data with increased reliability.

15. SUBJECT TERMS

Molecular dynamics, Particle-surface, Chemical sputtering, Erosion

16. SECURITY CLASSIFICATION OF:			17. LIMITATION OF ABSTRACT	18. NUMBER OF PAGES	19a. NAME OF RESPONSIBLE PERSON
a. REPORT	b. ABSTRACT	c. THIS PAGE			Dr. Donald L. Thompson, PI
U	U	U	U	7	19b. TELEPHONE NUMBER *(Include area code)* 573-882-0051

Reset

Standard Form 298 (Rev. 8/98)
Prescribed by ANSI Std. Z39.18

INSTRUCTIONS FOR COMPLETING SF 298

1. REPORT DATE. Full publication date, including day, month, if available. Must cite at least the year and be Year 2000 compliant, e.g. 30-06-1998; xx-06-1998; xx-xx-1998.

2. REPORT TYPE. State the type of report, such as final, technical, interim, memorandum, master's thesis, progress, quarterly, research, special, group study, etc.

3. DATES COVERED. Indicate the time during which the work was performed and the report was written, e.g., Jun 1997 - Jun 1998; 1-10 Jun 1996; May - Nov 1998; Nov 1998.

4. TITLE. Enter title and subtitle with volume number and part number, if applicable. On classified documents, enter the title classification in parentheses.

5a. CONTRACT NUMBER. Enter all contract numbers as they appear in the report, e.g. F33615-86-C-5169.

5b. GRANT NUMBER. Enter all grant numbers as they appear in the report, e.g. AFOSR-82-1234.

5c. PROGRAM ELEMENT NUMBER. Enter all program element numbers as they appear in the report, e.g. 61101A.

5d. PROJECT NUMBER. Enter all project numbers as they appear in the report, e.g. 1F665702D1257; ILIR.

5e. TASK NUMBER. Enter all task numbers as they appear in the report, e.g. 05; RF0330201; T4112.

5f. WORK UNIT NUMBER. Enter all work unit numbers as they appear in the report, e.g. 001; AFAPL30480105.

6. AUTHOR(S). Enter name(s) of person(s) responsible for writing the report, performing the research, or credited with the content of the report. The form of entry is the last name, first name, middle initial, and additional qualifiers separated by commas, e.g. Smith, Richard, J, Jr.

7. PERFORMING ORGANIZATION NAME(S) AND ADDRESS(ES). Self-explanatory.

8. PERFORMING ORGANIZATION REPORT NUMBER. Enter all unique alphanumeric report numbers assigned by the performing organization, e.g. BRL-1234; AFWL-TR-85-4017-Vol-21-PT-2.

9. SPONSORING/MONITORING AGENCY NAME(S) AND ADDRESS(ES). Enter the name and address of the organization(s) financially responsible for and monitoring the work.

10. SPONSOR/MONITOR'S ACRONYM(S). Enter, if available, e.g. BRL, ARDEC, NADC.

11. SPONSOR/MONITOR'S REPORT NUMBER(S). Enter report number as assigned by the sponsoring/ monitoring agency, if available, e.g. BRL-TR-829; -215.

12. DISTRIBUTION/AVAILABILITY STATEMENT. Use agency-mandated availability statements to indicate the public availability or distribution limitations of the report. If additional limitations/ restrictions or special markings are indicated, follow agency authorization procedures, e.g. RD/FRD, PROPIN, ITAR, etc. Include copyright information.

13. SUPPLEMENTARY NOTES. Enter information not included elsewhere such as: prepared in cooperation with; translation of; report supersedes; old edition number, etc.

14. ABSTRACT. A brief (approximately 200 words) factual summary of the most significant information.

15. SUBJECT TERMS. Key words or phrases identifying major concepts in the report.

16. SECURITY CLASSIFICATION. Enter security classification in accordance with security classification regulations, e.g. U, C, S, etc. If this form contains classified information, stamp classification level on the top and bottom of this page.

17. LIMITATION OF ABSTRACT. This block must be completed to assign a distribution limitation to the abstract. Enter UU (Unclassified Unlimited) or SAR (Same as Report). An entry in this block is necessary if the abstract is to be limited.

Nuclear Instruments and Methods in Physics Research B 267 (2009) 704–710

Contents lists available at ScienceDirect

Nuclear Instruments and Methods in Physics Research B

journal homepage: www.elsevier.com/locate/nimb

Plasma-surface interactions of hydrogenated carbon

P.S. Krstic [a,*], C.O. Reinhold [a], S.J. Stuart [b]

[a] Physics Division, Oak Ridge National Laboratory, P.O. Box 2008, Oak Ridge, TN 37831-6372, USA
[b] Department of Chemistry, Clemson University, Clemson, SC 29634, USA

ARTICLE INFO

Article history:
Received 6 October 2008
Received in revised form 31 October 2008
Available online 10 December 2008

PACS:
68.49.Bc
34.35.+a
68.49.Sf
52.40.Hf
61.80.X

Keywords:
Molecular dynamics
Particle-surface
Chemical sputtering
Erosion

ABSTRACT

We present a review of our study of interactions of plasma particles (atoms, molecules) with hydrogenated amorphous carbon surfaces typical of plasma-facing divertor tiles and deposited layers in magnetic-fusion reactors. Our computer simulations of these processes are based on classical molecular dynamics simulations, using the best currently available multibody bond-order hydrocarbon potentials. Our research in this field has been focused on the chemical sputtering of carbon surfaces at low impact energies, the most complex of the plasma-surface interactions (PSI). Close collaboration with beam-surface and plasma-surface experiments provides not only theoretical support for the experiments, but also builds suitable benchmarks for our methods and codes, enabling production of theoretical plasma-surface data with increased reliability.

1. Introduction

Since plasma-boundary physics encompasses some of the most important unresolved issues in future energy production for fusion reactors, there is a strong interest in the fusion community for better understanding and characterization of plasma-surface interactions (PSI). Chemical and physical sputtering cause the erosion of the limiter/divertor plates and vacuum-vessel walls, whether these are made of C, Be, W, or some combination (i.e. mixed materials), and degrade fusion performance by diluting the fusion fuel and excessively cooling the core. Hydrocarbon re-deposition onto plasma-facing components can lead to long term accumulation of large in-vessel tritium inventories.

A major challenge in the production of D–T fusion power is the development of materials for the first wall and internal components. The choice of wall material has profound effects on confinement of fusion-grade plasmas. Although carbon-based materials have superior thermo-mechanical properties, they could trap high levels of tritium by co-deposition with eroded carbon and thereby severely constrain plasma operations. Thus, a mix of several different plasma-facing materials is now proposed in ITER to optimize the requirements of areas with different power and particle flux characteristics. The slow rate of progress in the area of tritium removal, together with favorable results from divertor tokamaks with high atomic number (e.g. tungsten) walls, suggest that interest in all-metal machines will increase.

The key issues for surface experiments on carbon-based materials are erosion, reflection, impurity transport in the plasma, deposition, T uptake and removal. There is a need to determine the composition of eroded species such as hydrocarbon molecules and radicals, their rovibrational state and energy spectra, and their sticking coefficients to surfaces as a function of energy. An expansion of the available erosion database towards very low energies (5 eV) is needed in order to narrow the gap in erosion data between energetic hydrogen ions and thermal atomic hydrogen, both for pure carbon as well as mixed materials systems. Properly benchmarked molecular dynamics (MD) simulations could provide comprehensive databases for boundary plasma modeling, providing details often not accessible by experiment.

Chemical sputtering is a process where bombardment by atoms or molecules induces a chemical reaction which produces a particle that is weakly bound to the surface and hence is easily desorbed into the gas phase [1]. For carbon surfaces, it is hypothesized that incident particles break bonds within the collision cascade [2]. The broken bonds are rapidly passivated by the abundant flux of atomic hydrogen from the hydrogen fusion plasma environment. This leads to the formation of stable hydrocarbon molecules

* Corresponding author. Tel.: +1 865 574 4701; fax: +1 865 574 1118.
E-mail address: krsticp@ornl.gov (P.S. Krstic).

0168-583X/$ - see front matter © 2008 Elsevier B.V. All rights reserved.
doi:10.1016/j.nimb.2008.11.049

underneath the surface, which diffuse to the surface and desorb thermally.

In our MD simulations the classical motion of a collection of atoms is followed using forces obtained from predefined analytic ground electronic state potentials, which for hydrocarbon systems have reached maturity (empirical bond-order potentials of the Tersoff–Brenner type, such as REBO [3,4] and AIREBO [5]) and their predictive strength is improving. The parameters of the phenomenological potential functions are taken either from parameter-free quantum-mechanical calculations or experimental data. Dynamic electronic effects are not included in classical MD. Non-local effects, which take into consideration the bonding structure further away than the nearest neighboring atoms, may be included in the potential to improve the accuracy of the calculations. This is especially important for carbon, where heterogeneous bonding configurations arise from the presence of hybridized bonding. The REBO potential has a reasonably realistic description of pure carbon and hydrocarbon molecular structures, as well as dynamic effects, such as bond forming and breaking. Hence, it has been adopted by most MD studies of sputtering [6–9] including our own [10–15]. The AIREBO potential overcomes some limitations of the REBO potential, but requires significantly faster computer resources, due to the longer range of the potential.

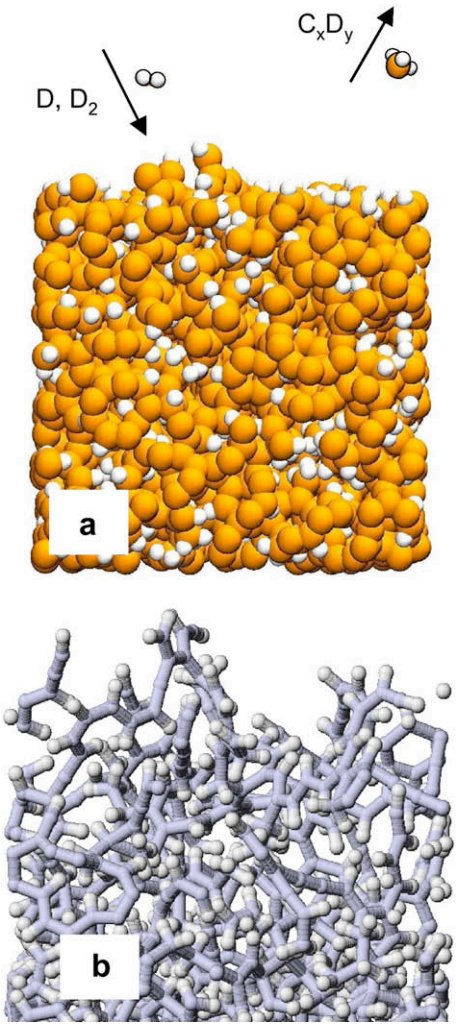

Fig. 1. (a) Chemical sputtering upon impact of D and D_2 projectiles on deuterated amorphous carbon and (b) filamentous low-density structures at the interface after prolonged bombardment with 20 eV D.

The numerical cell must be larger than the characteristic region of atom impact induced perturbation, to secure scattering-free cell boundaries. In the range we have studied [10–15], below 30 eV impact energy, a realistic cell of deuterated carbon consists of a cubic random C:D network of several thousand atoms, with edge dimension of 2.5 nm (Fig. 1(a)) and two-dimensional periodic boundary conditions in the planes perpendicular to the surface plane. Saturated surfaces are prepared by cumulative bombardment of several thousand projectiles during creation times up to 10 ns until a saturation regime is reached [10,15]. Cumulative bombardment not only erodes the surface, but also creates surface swelling producing a lower-density interface that is inhomogeneous and contains filamentous structures [14] of hydrocarbon chains (Fig. 1(b)), which play an important role in the PSI dynamics. Bombardment also changes the D/C ratio close to the surface interface (extending to increasing depths with increasing impact energy), where it reaches values $\geqslant 1$, as seen in Fig. 2. Sputtering yields typically reach a nearly stationary regime as a function of fluence. However, this stationarity can never be a true steady-state since the finite simulation cell is continually changing due to erosion. In any case, chemical sputtering is strongly dependent on the accumulation of hydrogen in the surface and, consequently, depends on the concentration of carbon atoms with $sp/sp^2/sp^3$ hybridization states, which also changes with fluence. This explains the change in the total carbon yield as a function of the deuterium fluence, shown in Fig. 3, which is also seen experimentally [16]. Most of our simulations were done with surfaces prepared in the range of 1000–2000 impacts (at or beyond the point where the sputter yield has reached an approximate stead state in Fig. 3).

After creating the surfaces by cumulative bombardment, sputtering yields are subsequently calculated by independent random impacts of several thousand projectiles on the saturated surfaces [10]. At the lowest energies the time duration of the collisional cascade for each impact is less than 5 ps, but approaches 30 ps for 30 eV deuterium impacts [15]. Calculations are performed using 2000–4000 independent trajectories for 5–30 ps. Such level of statistics is essential for meaningful calculation of small yields. Our recent calculations [10–15] of impact of deuterium atoms and molecules have shown good agreement with the experimental results [17] for sputtering of methane and acetylene. This good agreement for selected hydrocarbon yields is the result of our computational methodology: we mimic the cumulative saturation conditions of

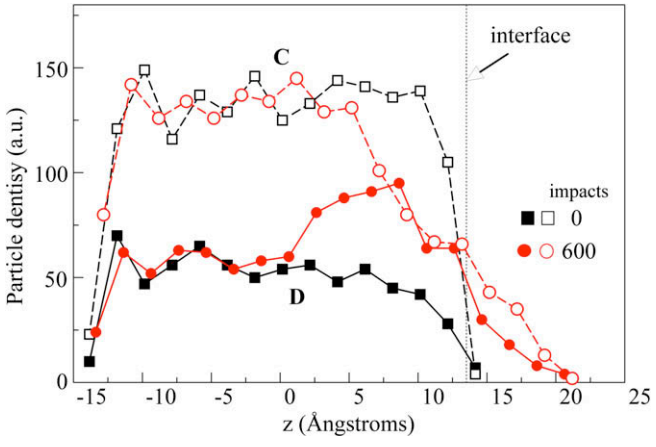

Fig. 2. Depth profile for the density of carbon (open symbols) and deuterium (solid symbols) in the simulation cell, both for the initial surface (black squares) and for the surface after 600 impacts (red circles). Initially, the cell was created from a random distribution with a D/C ratio of 0.4, homogenized by a heating and annealing. (For interpretation of the references to color in this figure legend, the reader is referred to the web version of this article.)

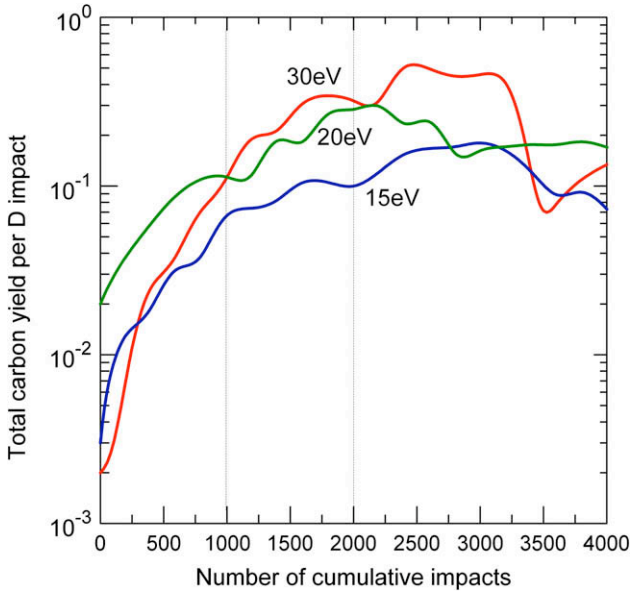

Fig. 3. Evolution of carbon yield with increasing D fluence in the process of surface preparation.

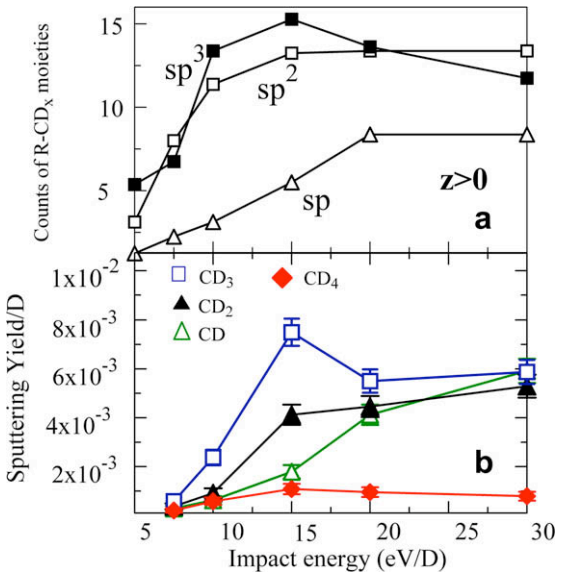

Fig. 4. (a) Counts of R-CDx moieties in the simulation cell as a function of impact energy, integrated over the portion of the simulation cell with $z > 0$, for a range of impact energies. The counts represent averages across six surfaces [10]. (b) Sputter yield of CD_x hydrocarbons.

the beam-surface experiment as closely as possible, preparing the surface self-consistently by bombardment with appropriate particles at appropriate energies, until a quasi steady-state regime in the sputtering yields is reached [10]. This results in hundreds of prepared surfaces, for various energies and impact particles, which are then used in the computational simulations of chemical sputtering, repeated for each case thousands of times, and averaged over a number of surfaces, obtained at various fluences. We have calculated particle, energy and angular spectra of the sputtered hydrocarbons, reflection coefficients, penetration coefficients, dissociation probabilities of impacting D_2, and D_2 production at the surface with impact of D [15]. We have also shown that the sputtering yields of hydrocarbons strongly depend on the initial vibrational states of impacting D_2 molecules [11].

In addition to particle beams, well-controlled plasma sources can also be used for experimental characterization of sputtering processes. Experiments of this kind were performed recently [18] for the accommodation coefficients of H_2 interacting with polycrystalline carbon surfaces. We have therefore calculated the sputtering yields and reflection coefficients using a distribution of impacting particles that mimics a plasma environment, which can be directly validated by experiment.

In the following we present a brief review of typical results obtained in our simulations of surface irradiation with particle beams and new results with the plasma-irradiated surfaces.

2. Results

Most of our results were obtained under the assumption of a monoenergetic beam irradiation, incident perpendicular to the surface, which is kept at temperature of 300 K using a Langevin thermostat (for details see [10–15,17]). We have studied the least well known, intermediate-to-low range of impact energies (1–30 eV/D), with D and D_2 projectiles impacting deuterated amorphous carbon surfaces.

2.1. Chemical sputtering and surface microstructure

Assuming the bond breaking as the first step in the chemical sputtering process, hydrocarbon moieties R-CD_x at the interface which are created at the terminal-ends of the branched network structure are expected to play a dominant role in the sputtering of the simplest hydrocarbons, like CD, CD_2 and CD_3. Furthermore, the sputtering yield dependence of these hydrocarbons on impact energy should be proportional to the corresponding densities of *sp*, sp^2 and sp^3 terminal carbons, respectively, generated in the surface at the various sputtering yields. Our simulations show striking similarities between the shapes of the relevant yields and the sp^x densities as functions of the impact energy/D (Fig. 4), confirming that the leading mechanism for the CD_x sputtering is the bond breaking of terminal-end R-CD_x moieties [10].

2.2. Vibrational excitation of the impinging molecules [11]

The impacting particle is most efficient in chemical sputtering at the end of its thermalization cascade. Penetration of an impacting molecule (like D_2) into a hydrogenated carbon surface might be suppressed due to the molecule physical dimensions. Thus, the dissociation of the molecule is a predecessor for the successful chemical sputtering. However, depending on the vibrational excitation of the D_2 molecule, a fraction of the impact energy must be expended for the dissociation, which depends on how highly the molecule is excited. Therefore, the sputtering yield increases with increasing vibrational excitation, as shown in Fig. 5, as function of the classical vibrational amplitude of the D_2 molecule. The maximum is reached at the end of the correlation distance of the short range REBO potential, about 2 Å. Beyond the maximum, when the atoms are not directly correlated, the sputtering yield decreases slightly since the interaction between the two impact cascades decreases with distance. When the distance between the impacting atoms becomes large enough, the sputtering yield tends to twice the single D-atom yield, also shown in Fig. 5.

2.3. Validation of the MD simulation: comparison with the beam experiments

By mimicking experiments through preparation of the surfaces self-consistently in energy and particle type by cumulative bombardment, very good agreement was obtained between the MD

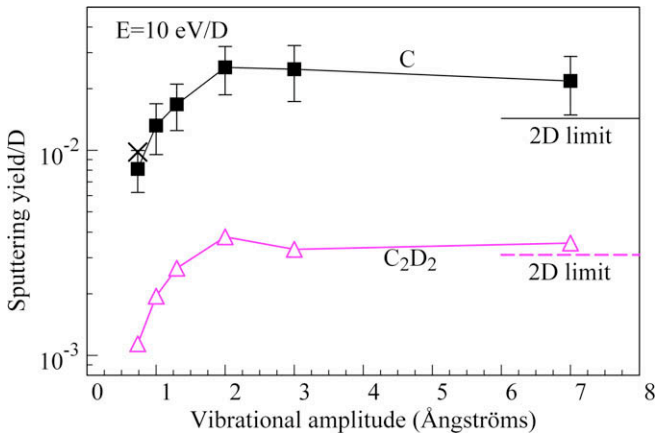

Fig. 5. Calculated sputtering yields per deuterium atom of acetylene (C_2D_2, open triangles) and total carbon (filled squares) for a D_2 impact energy of 10 eV/D, as a function of the initial internal vibrational state of D_2, expressed through the maximum "bond" length (classical vibration amplitude), λ [11]. The yields for impact of non-interacting D are multiplied by a factor of two and are shown by the rightmost horizontal lines.

simulation results for the methyl + methane sputtering yield and measurements of the ejected methane yield [10,17] (Fig. 6). We note that the experimental results in Fig. 6 correspond to incident D_2^+, which could be mimicked by two D atoms (see Fig. 5) if the D_2, obtained by neutralization of the D_2^+ above the surface, is in a highly vibrationally excited state. It is not currently clear what is the role of the post-sputtering processes in the experimental chamber, nor whether our simulation contains a complete description of methane production. However, it is of no concern that the measurements were done with D_2^+ or D^+, and simulations with D_2 (or with D): The neutralization of D_2^+ is expected to happen through resonant charge transfer to vibrationally excited D_2 [11], and neutralization of D^+ goes through resonant charge transfer to D, which are very fast processes in both cases.

2.4. Mass spectra of the ejected hydrocarbons [10,12,15]

The preparation of the surfaces by cumulative bombardment at each energy and particle type turned out to be essential for sputtering of complex hydrocarbons [10]. A "virgin" surface has the tendency to eject only carbon atoms and diatoms, and the very simplest hydrocarbons (like CH). Fig. 7 shows the mass spectra of hydrocarbons, ejected in MD simulations by vibrationally excited

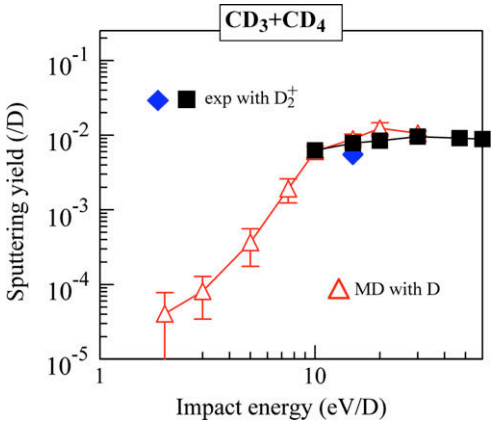

Fig. 6. Comparison of the MD result for sputtering of $CD_3 + CD_4$ by D impact with the results of beam experiments for D_2^+ impact [19].

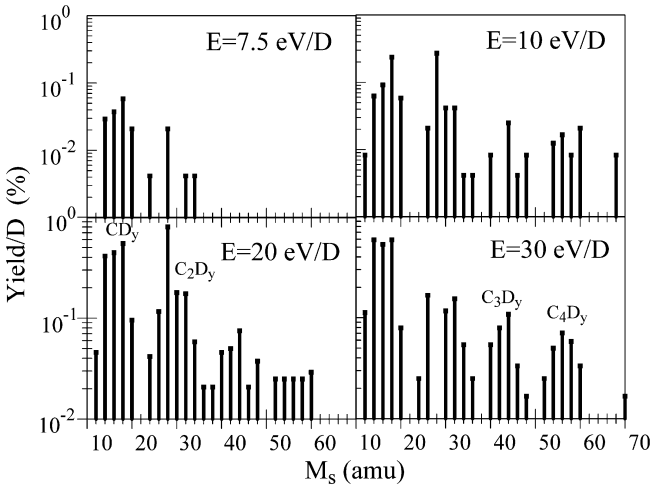

Fig. 7. Yields of hydrocarbons, sputtered by D_2 impact on a–C:D, as functions of mass of the ejected molecules, for various impact energies [10,12].

D_2. The groups C_xD_y are well separated in x. With increasing impact energy, more and more complex hydrocarbons arise. While at the lowest energies mostly $x = 1$ hydrocarbons are sputtered, at 30 eV/D hydrocarbons with up to $x = 4$ are visible in the mass spectrum. The distribution of the ejected hydrocarbons is not uniform with y for a given x but peaks at progressively less saturated hydrocarbons with increasing mass. For $x = 1$ the biggest yield is of methyl, CD_3, for $x = 2$ it is for acetylene, C_2D_2, for $x = 3$ the maximum is at C_3D_4, and so on.

2.5. Energy spectra of the hydrocarbons [10,12,15]

Energies of the ejected hydrocarbons as function of their mass, for various values of the impact D_2 energy, are shown in Fig. 8. Although the dispersion of energies seems to decrease with mass, it is rather counterintuitive that both light and heavy ejected particles have similar average energies, irrespective of the impact energy. These average values are between 0.5 and 1 eV, and are too energetic to arise thermally from the surface at 300 K. An explanation is that sputtering is a kinetic process, i.e. a hydrocarbon is ejected by a chemical processes at the end of the collisional cascade [10]. The sputtered particle is thermalized with the locally

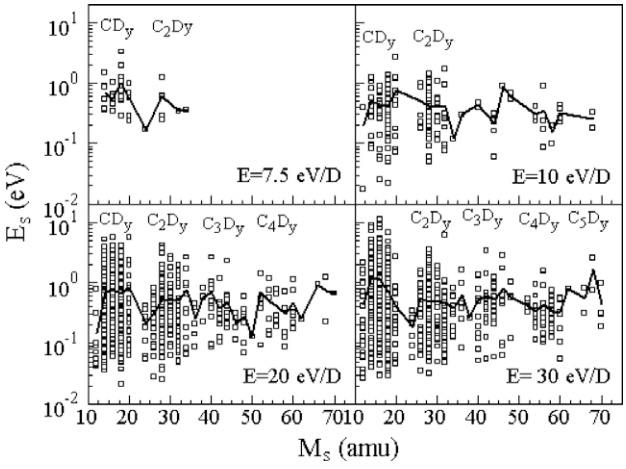

Fig. 8. Energy spectra of ejected hydrocarbons as functions of hydrocarbon mass [10,12]. Each point indicates an individual ejecta. The solid line represents the average at each mass number.

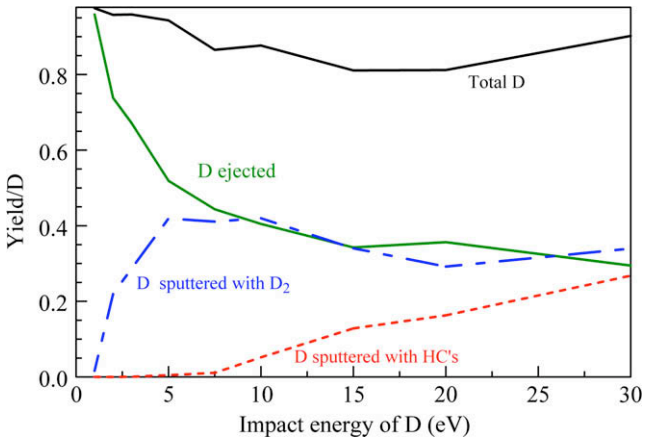

Fig. 9. Yields of D, D in D_2 and D in hydrocarbons, and their sum (total D) for various impact energies of atomic D at normal incidence [15].

elevated temperature, which is confirmed by the Maxwell-Boltzmann distribution of the ejected particles [10,15].

2.6. Balance of various channels of hydrogen ejection [10,15]

Deuterium is ejected in the form of reflected (and sputtered) atoms, as well as in the form of sputtered D_2 and hydrocarbons (Fig. 9). At impact energies in the range 4–5 eV, there is a change in trends of the curves in Fig. 9 which corresponds to the covalent bond dissociation energy in a-C:D. Above 5 eV, the reflection coefficient continues to decrease, although much more slowly. A larger fraction of the D-atoms is retained in the substrate at higher energies. The D_2 yield is largest at 5–10 eV and decreases gradually as the impact energy increases above 10 eV. The continued decrease in D reflection is due both to the increased D retention (implantation) as well as growth in the yield of hydrocarbons that carry off multiple D-atoms.

In presence of erosion, one might even expect that total ejection yield of hydrogen (in all channels) could be even larger than 1. This does not happen here, indicating that the surface is accreting hydrogen faster than it is eroding at these fluences. There is erosion of carbon, which increases with impact energy, but the yield of hydrocarbons stays low (as is well known).

2.7. Angular distribution of ejecta [10,15]

Because the target is amorphous and we only consider D impacts normal to the surface, the angular distributions $dN/d\Omega_P$ are independent of the azimuthal angle in the plane of the surface interface. Therefore, for the center of mass (c.m.) momentum P of the ejected particle, only the dependence on the polar angle θ_P with respect to the surface normal, is of interest.

The angular distributions for sputtered D_2 and hydrocarbons, for various impact energies of D are presented in Fig. 10 [15]. For physical sputtering and normal incidence on an amorphous solid the angular distributions of the ejected momenta are expected to follow $dN/d\Omega_P \sim \cos\theta_P$. The present distributions for chemical sputtering approximately mimic this behavior, particularly at high energies although the curves are somewhat more sharply peaked around ejection normal to the surface than $\cos\theta_P$.

2.8. Rovibrational spectra of sputtered molecules [15]

Rotational, vibrational and rovibrational energies of ejected D_2 and hydrocarbons are presented in Fig. 11 as functions of the impact energy of D. The features of the curves in the range of

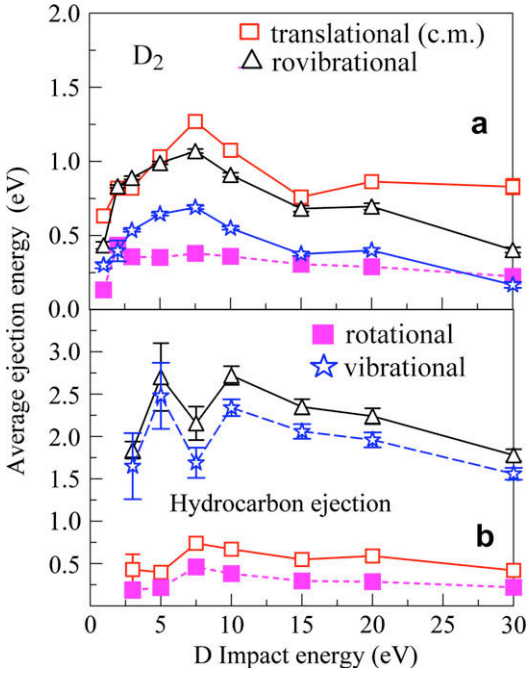

Fig. 11. Average ejection energy, including internal energy (vibrational and rotational) of ejected molecules by D impact, for ejected: (a) D_2 and (b) hydrocarbons [15].

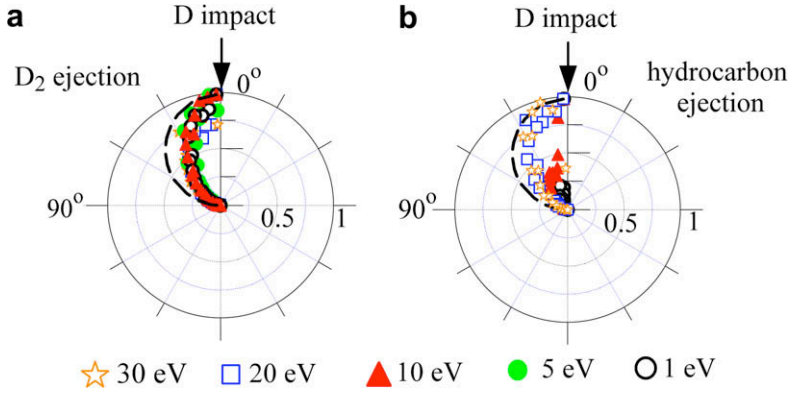

Fig. 10. Angular distributions of the c.m. momentum of ejected molecules upon D impact [15] as a function of the polar angle θ_P with respect to the surface normal. The thick dashed lines represent an angular distribution $dN/d\Omega_P \sim \cos\theta_P$. The distributions are normalized such that the maximum values of $dN/d\Omega$ lie on the unit circle.

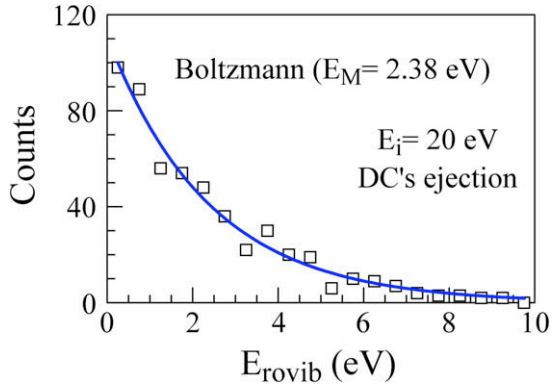

Fig. 12. Rovibrational energy distribution of emitted hydrocarbons following 20 eV D impact. The line is a Boltzmann distribution $\sim\exp(-E/E_M)$.

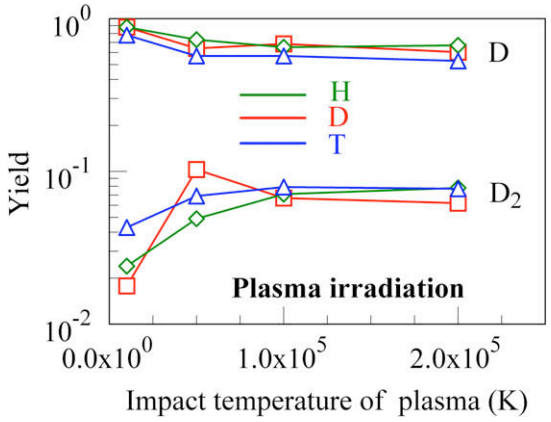

Fig. 13. Isotope specific yields of H (D, T) atoms and H_2, (D_2, T_2) molecules upon irradiation by plasmas composed of H (green squares), D (red squares), or T (blue squares) at various temperatures. Random impacts were used both in preparation of the surfaces and in calculation of the sputter yield. The target surface was kept at a temperature of 300 K. (For interpretation of the references to color in this figure legend, the reader is referred to the web version of this article.)

5–10 eV impact energy reflect the C–D and C–C bond breaking energy in 4–5 eV range. The translational energies of ejected molecules are in range of 0.5–1 eV. In the same interval are rovibrational energies of D_2 (Fig. 11(a)), approximately equipartitioned between rotational and vibrational energies, especially at the higher end of impact energies. In turn, rovibrational energies of hydrocarbons are significantly higher than translational energies, about 2 eV, mostly due to the increased number of vibrational modes of the complex molecules. Of course, the corresponding temperatures per degree of freedom are closer to the rotational and translational temperatures, in the range of 5000 K. As can be seen from Fig. 12, the motion of ejecta is at least approximately thermalized at an elevated temperature, similarly to the translational motion of the ejected molecules [10].

2.9. "*Plasma*" *irradiation*

Simulations have shown that it is important to properly mimic the experimental conditions and history. For a surface exposed to a plasma this includes bombarding the surface with random angles and energy energies of impact. We mimic a plasma by randomly sampling the impinging energies of hydrogen, deuterium and tritium atoms from a Maxwell distribution, and the impact angles from a uniform distribution. Here, we show preliminary results, which acquired enough statistical weight only for atom reflection and sputtering of hydrogen molecules. Each surface used as a target was prepared self-consistently by randomized cumulative irradiation with a large number (1000–2000) of like atoms, at a desired plasma temperature. Results for ejection of impact-like particles and sputtering of impact-like diatomic molecules are shown in Fig. 13, for a range of sampled temperatures 10,000–200,000 K (0.86–17 eV). It is interesting to note that the reflection yield stays (independent of the isotopic composition) at the highest temperatures in the range 0.5–0.6 after the initial decline, somewhat higher than that for the normal-beam irradiation (Fig. 9) at the highest energies. This is due to the averaging over impinging angles and energies that takes place for a plasma-surface interaction. For the same reason sputtering yields of hydrogen molecules stay below 0.1, increasing slightly with isotopic mass. In contrast to what is expected for carbon erosion, the yields for H and H_2 ejection are nearly independent of the mass of the projectile. Fig. 14 displays the average energies of the ejected particles as functions of the impact temperature and shows that they are, within the statistical uncertainty, similar for all three impact isotopes. While the "reflected" energies follow the impact ones almost elastically, the energy of the sputtered molecules stays constant, as in case of beam irradiation (Fig. 11).

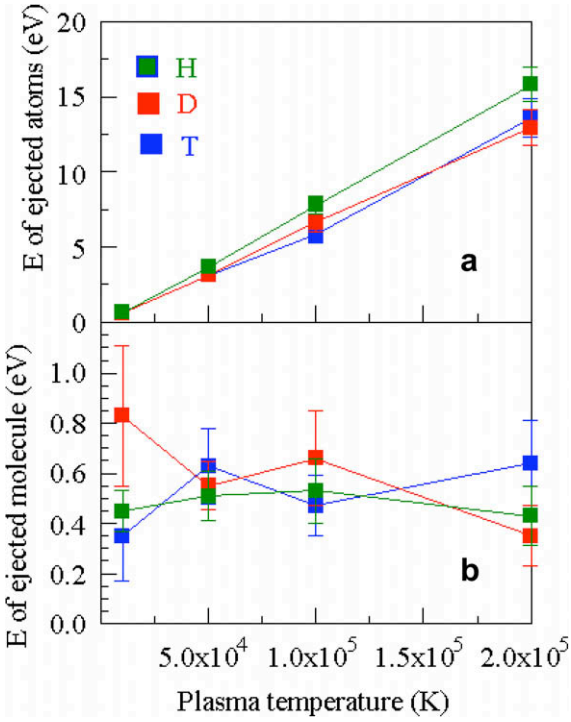

Fig. 14. Translational energy spectra of ejected particles upon irradiation as described in Fig. 13.

3. Outlook

The need for the new materials in fusion, ITER in particular, requires studies of not only new forms of carbon (including variations of the C crystalline and polycrystalline structures, CFC, and C doped with boron and beryllium) but also conceptually new materials like tungsten and beryllium and their compounds and alloys mutually and with carbon and hydrogen. Results from plasma irradiating particles, like $N(N_2)$, C, W, Be, inert gases, as well as isotopic effects of impacting hydrogen are needed for a more complete understanding of interactions of fusion plasma with plasma-facing materials.

To satisfy these needs, development of new potentials that would include C, W, Be, and H is a basic prerequisite. Further development of the hydrocarbon potentials to improve the reaction dynamics and chemistry of complex hydrocarbons and doped carbon is also needed. The fast expansion of computation capabilities toward petascale machines might also provide the capability for more realistic simulations in the development of new methods, including a direct quantum-mechanical computation of the required potentials, introducing electronic excitations and charge transfer during the impact cascade into the MD simulations.

Acknowledgments

We acknowledge support by the OFES (PSK) and OBES (COR) of the US DoE under Contract No. DE-AC05-00OR22725 with UT-Battelle, LLC, and partial support through SciDAC and DoE INCITE project SC18392. SJS acknowledges support by the DoE (No. DE-FG02-01ER45889), NSF (No. CHE-0239448) and the DOD (No. 47539-CH-MUR).

References

[1] W. Jacob, J. Roth, Chemical sputtering, in: R. Behrisch, W. Eckstein (Eds.), Topics in Appllied Physics, Vol. 110, Springer-Verlag, Berlin, Heidelberg, 2007, p. 329.
[2] E. Salonen, K. Nordlund, J. Keinonen, C.H. Wu, Phys. Rev. B 63 (2001) 195415.
[3] D.W. Brenner, Phys. Rev. B 42 (1990) 9458.
[4] D.W. Brenner, O.A. Shenderova, J.A. Harrison, S.J. Stuart, B. Ni, S.B. Sinnott, J. Phys.: Cond. Matt. 14 (2002) 783.
[5] S.J. Stuart, A.B. Tutein, J.A. Harrison, J. Chem. Phys. 112 (2000) 6472.
[6] E. Salonen, Ph.D Thesis, University of Helsinki Report Series in Physics, HU-P-D97, 2002. <http://ethesis.helsinki.fi/>.
[7] J. Marian, L.A. Zepeda-Ruiz, G.H. Gilmer, E.M. Bringa, T. Rognlien, Phys. Scr. T124 (2006) 65.
[8] P. Träskelin, K. Nordlund, J. Keinonen, J. Nucl. Mater. 357 (2006) 1.
[9] J. Marian, L.A. Zepeda-Ruiz, N. Couto, E.M. Bringa, G.H. Gilmer, P.C. Stangeby, T.D. Rognlien, J. Appl. Phys 101 (2007) 044506.
[10] P.S. Krstic, C.O. Reinhold, S.J. Stuart, New J. Phys. 9 (2007) 209.
[11] P.S. Krstic, C.O. Reinhold, S.J. Stuart, Europhys. Lett. 77 (2007) 33002.
[12] P.S. Krstic, S.J. Stuart, C.O. Reinhold, AIP Conf. Proc. 876 (2006) 201.
[13] C.O. Reinhold, P.S. Krstic, S.J. Stuart, Nucl. Instr. and Meth. B 258 (2007) 274.
[14] S.J. Stuart, P.S. Krstic, T.A. Embry, C.O. Reinhold, Nucl. Inst. and Meth. B 255 (2007) 202.
[15] P.S. Krstic, C.O. Reinhold, S.J. Stuart, J. Appl. Phys. 104, in press.
[16] L.I. Vergara, F.W. Meyer, H.F. Krause, J. Nucl. Mater. 347 (2005) 118.
[17] F.W. Meyer, P.S. Krstic, L.I. Vergara, H.F. Krause, C.O. Reinhold, S.J. Stuart, Phys. Scr. T128 (2007) 50.
[18] E.M. Hollmann, P.S. Krstic, R.P. Doerner, D. Nishijima, A. Yu Pigarov, C.O. Reinhold, S.J. Stuart, Plasma Phys. Contr. Fus. 50 (2008) 102001.
[19] H. Zhang, F.W. Meyer, H.M. Meyer III, M.J. Lance, Vacuum 82 (2008) 1285.